Accepted Manuscript

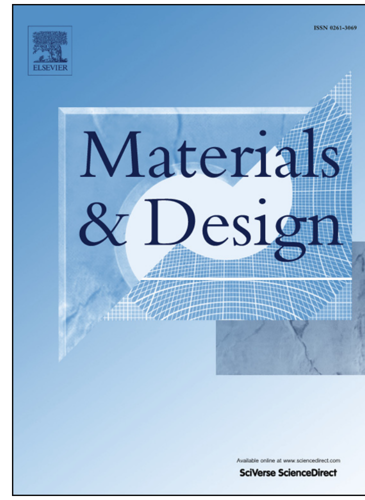

Effect of substrate temperature on the interface bond between support and substrate during selective laser melting of Al-Ni-Y-Co-La metallic glass

X.P. Li, M. Roberts, Y.J. Liu, C.W. Kang, H. Huang, T.B. Sercombe

PII: S0261-3069(14)00681-5
DOI: http://dx.doi.org/10.1016/j.matdes.2014.08.065
Reference: JMAD 6762

To appear in: *Materials and Design*

Received Date: 11 July 2014
Accepted Date: 26 August 2014

Effect of substrate temperature on the interface bond between support and substrate during selective laser melting of Al-Ni-Y-Co-La metallic glass

X.P. Li [a,*], M. Roberts [b], Y.J. Liu [c], C.W. Kang [d], H. Huang [d] and T.B. Sercombe [a]

[a] The University of Western Australia, School of Mechanical and Chemical Engineering, Perth, WA 6009, Australia

[b] The University of Western Australia, Centre for Microscopy, Characterisation and Analysis, Perth, WA 6009, Australia

[c] Edith Cowan University, School of Mechanical Engineering, Perth, WA 6027, Australia

[d] The University of Queensland, School of Mechanical and Mining Engineering, Brisbane, QLD 4072, Australia

[*] Corresponding author email: xiaopeng.li@uwa.edu.au ; Telephone: +61 8 6488 3220

Abstract: An Al-Ni-Y-Co-La metallic glass was laser-melted onto an Al substrate which was at two different temperatures: 25℃ and 250℃. It was found that the substrate temperature played a critical role in determining the interface bonding between substrate and support and final solidification microstructures. The higher substrate temperature resulted in the formation of a stronger interface bond between metallic glass and substrate while lower substrate temperature resulted in the formation of a weaker interface bond. This has been attributed to different cooling rates and thermal histories present in the two cases. A multi-physics-based computational model based on the heat transfer theory in heat transient mode of COMSOL™ was introduced to explain the underlying mechanism.

Keywords: Selective laser melting; Metallic glass; Interface; Solidification microstructure; Nanoindentation

1. Introduction

Selective laser melting (SLM) has undergone a rapid development for a decade [1]. As an emerging additive manufacturing technique, it shows great potential in fabrication of metal components with complex geometries, unachievable through conventional manufacturing techniques [1]. Due to its net-shape formation capability and high freedom of customer design ability, potential applications of SLM in medical implants, aircraft and automobile industries have been foreseen and are becoming promising [1-3]. SLM is characterised by very high heating and cooling rates which can reach 10^3-10^8 K/s [4, 5]. Due to its unique and advantageous "point-by-point" processing, only a small volume of material is heated as the laser beam travels across the powder bed. This leads to the possibility of not only obtaining non-equilibrium microstructures, but also as a promising alternative for the production of large-size bulk metallic glass (BMG) and composites [6-8].

Similar to the fabrication of crystalline alloys via SLM, the high heating and cooling rate experienced during SLM of metallic glass can cause high temperature gradients and thermal fluctuations to occur. This results in severe and detrimental thermal and residual stresses to form [8-10]. These stresses will tend to result in curling, cracking or even delamination of the fabricated BMG components [8]. The formation of residual stresses is particularly important in BMG materials due to their intrinsic brittleness. To counteract these stresses, BMG parts made by SLM must be attached to a base plate using a support structure. The interface between the support and substrate is critical in determining the final success of the BMG part and some of the authors' preliminary trials show that the curling, cracking and delaminating of the fabricated BMG components always happen at the interface between the support and the substrate. As such, it was necessary to study the bond between these two regions, especially the influence of the substrate temperature. However, to the knowledge of the authors, this has not been reported yet.

In this work, a recently developed Al-based metallic glass was melted onto a pure Al substrate using SLM. The influence of substrate temperature on the interface bond between support and substrate and solidification microstructure was studied. Results show that the higher substrate temperature gave rise to stronger bond between the metallic glass and substrate. In addition, the solidification microstructure of the material is strongly affected by the substrate temperature, which has been attributed to the different cooling rates and thermal histories. This study provides a fundamental basis for successful fabrication of BMG components via SLM.

2. Experimental details

Master ingot with a nominal composition of $Al_{86}Ni_6Y_{4.5}Co_2La_{1.5}$ (in at. %) was prepared by arc melting high-purity elemental pieces Al (>99.9 wt. %), Ni (>99.9 wt. %), Y (>99.0 wt. %), Co (>99.9 wt. %) and La (>99.0 wt. %) under a Ti-gettered argon atmosphere for six times to ensure chemical homogeneity. Powder was then produced by nitrogen-atomisation and sieved to below 25 μm. The particle size was measured using a Malvern Mastersizer Plus. The morphology and particle size of the powder are shown in Fig. 1. Its amorphous nature was confirmed using X-ray diffraction (XRD) and transmission electron microscopy (TEM) in the authors' previous studies [11, 12]. SLM experiments were conducted using a ReaLizer SLM-100 machine (ReaLizer GmbH, Germany) which is equipped with a fibre laser, generating a laser beam with a wavelength of 1060 nm and maximum power of 200 W at the part bed. A high purity argon gas was used during the processing [13]. According to several preliminary trials [7], at a laser scan speed of 750 mm/s a high laser power (200 or 160 W) can cause severe crystallization and cracks during SLM of BMG while low laser energy (80 W) can also cause cracks. Hence, the laser scan speed and power in this study were set at 750 mm/s and 120 W, respectively. To investigate the interface between support and substrate, a 100 µm single layer of metallic glass powder was built on an Al substrate, which was either at room temperature (~ 25ºC) or had been heated to ~ 250ºC which is lower than the glass transition temperature (T_g) of the powder [12]. Scanning electron microscopy (SEM, Zeiss 1555 VP-FESEM, operated at an accelerating voltage of 15 kV and working distance 10 mm), electron probe microanalyser (EPMA, JEOL 8530F microprobe, equipped with 5 tuneable wavelength dispersive spectrometers operated at 40 degrees take-off angle, a beam energy of 15 keV and beam current of 20 nA for a dwell time per pixel of 20 ms) and nanoindentation (Hysitron® Triboindenter, at room temperature in air with a Berkovich indenter of a tip radius of 100 nm) were used to investigate the interface between the support and substrate and solidification microstructure of the support. The maximum indentation force applied was 2 mN at a rate of 200 µN/s for both loading and unloading. The dwell time at the peak load was fixed at 10 s. A minimum of 10 indentations were conducted on each site. A finite element modelling (FEM) method using a multi-physics-based computational model based on the heat transfer theory in heat transient mode of COMSOL™ [4] was used to estimate the cooling rates and temperature distribution during SLM.

3. Results and discussion

The interface between support and substrate with different substrate temperatures is shown in the back-scattered SEM images in Fig. 2. At a substrate temperature of 250℃ (Fig. 2a), there is a region with a sub-circular morphology (width ~ 100 µm and depth ~ 50 µm) that sits in between the support and the substrate. It is apparent that both the powder and top part of the substrate have been melted together and a good bond exists between the two. This sub-circular morphology is caused by the Gaussian distribution of the laser beam energy (TEM_{00}, $M^2 < 1.05$) and the competition between convection and conduction heat transfer within the melt pool, which has been explained in detail in the authors' previous study [7]. At room temperature there is no such sub-circular region between the support and substrate and a clear interface gap can be observed, as indicated by the white arrow in Fig. 2b. Although the heat generated from the laser seems to be sufficient to melt the powder, melting of the top of the substrate has not occurred. This suggests that the temperature at the interface does not exceed the melting point of the Al substrate (~ 660ºC). In addition, it can be seen that at a substrate temperature of 250ºC there is no apparent crystallization in the melt pool shown in Fig. 2c while severe crystallization has occurred in the melt pool after solidification, signified by the apparent crystalline phases shown in Fig. 2d. At the higher substrate temperature, there is a dark phase sitting at the interface between the support and substrate which is arrowed in Fig. 2a. Based on the SEM energy dispersive X-ray spectroscopy analysis (EDS) of this area shown in Fig. 3, it is apparent that this phase is an Al-rich oxide and has presumably formed during melting.

It is well acknowledged that convection in the melt pool plays a key role in heat transfer during laser processing especially when the laser energy density is high [7, 14]. This convection can also enhance mass transport during SLM, as material flows from the hotter centre of the melt pool to the edge, driven by the negative coefficient of surface tension of the metallic glass [15]. Since the laser-material interaction time is usually of the order of 100 μs and the melted materials exhibits rapid solidification, slow mass transfer mechanisms, such as diffusion, would have little effect on the formation of the bond between the metallic glass and substrate [16]. Therefore, it is believed that forming the bond in such a short time is mainly through convection-enhanced mass transport. To investigate this mass transport in the melt pool, EPMA was used to characterize the chemical distribution of the main elements Al, Ni, Y and Co in the abovementioned sub-circular interface region and the results are shown in Fig. 4. It is apparent that both the support and the melted substrate regions show a swirl-like pattern, most likely as a result of convection-enhanced mass transport. The swirling pattern is more apparent in the melted substrate region compared to the support region, indicating that the convection is stronger here. In addition, the lower part of the melt pool contains a higher concentration of Al and lower amounts of the other elements (Ni, Y and Co) than the support, which is likely to be a result of the melting of the aluminium substrate.

To investigate the reason and the underlying mechanism for the formation of this bonding region, the temperature distribution within the melt pool at the two substrate temperatures and the corresponding cooling rates during solidification were estimated based on a multi-physics-based computational model. For Al alloys, the laser absorption is very low ~5% at the 1μm wave length used [17]. Since there has been no published data on the laser absorption of Al-Ni-Y-Co-La metallic glass and the metallic glass in this study contains 86% Al, it was assumed to be similar to that of Al. Many factors such as the size and morphology of the powder particles will influence the actual absorption co-efficient of a material [18]. However, given that the substrate temperature is the only variable with all other parameters kept constant, including the powder used, there is not expected to be a significant change in the laser absorption between the two cases. For simplification, the simulation was carried out on Al-based thin film with the same composition as the powder this study used and no gap between the metallic glass and substrate was considered. The thickness of this thin film was set to 100 μm, which is identical to the actual thickness of powder deposited on the substrate. The results are shown in Fig. 5. It can be seen that the temperature distribution varies with the substrate temperature, signified by the isothermal line in Figs. 5a and b, which shows the melting point of Al. This contour line is an indication of the expected shape of the melt pool.

It is apparent from Fig. 5 that the area of material heated to above the melting point of aluminium is much greater at a substrate temperature of 250℃ than at room temperature. This difference explains why the melting of the Al substrate occurs at 250℃ rather than at room temperature. It is also apparent from Fig. 5, that the depth of the melting contour is larger than its width at both substrate temperatures and the difference is greater at 250℃ than at room temperature. According to the authors' previous study [7], this indicates that convection rather than conduction plays a dominant role in the heat transfer and higher substrate temperature can enhance the convection within the melt pool. These are consistent with the solidified microstructure shown in Figs. 2 and 4.

The heating and cooling rates at different points (I-V) in the melt pool are obtained from the model, shown in Fig. 5c. In both cases the cooling rate decreases along the vertical direction (from point I to V). At the centre of the melt pool (point I), the cooling rates at a substrate temperature of 250ºC and room temperature are similar and estimated to be 3.5×10^3 K/s and 3.6×10^3 K/s, respectively. These cooling rates are greater than the reported critical cooling rates R_c of this Al-based metallic glass (1.5×10^3 K/s)[12]. At the interface between the support and substrate (point III) the cooling rate on the unheated plate is greater (1.4×10^3 K/s) than when the substrate is heated to 250℃ (1.1×10^3 K/s). The difference in cooling rate between the two substrate temperatures becomes larger as you move vertically further away from the heat source.

The fact that the cooling rate is greater than the R_c should mean that the amorphous nature is retained after solidification [19]. From the model, the predicted cooling rates at both substrate temperatures are higher than the critical cooling rate of the Al-based BMG. This model is based on the condition that the heat can be transferred from support to the Al substrate without any obstruction. At a substrate temperature of 250℃, this is indeed correct, with no apparent crystallization occurring (Fig. 2a). However, this is not the case for the room temperature substrate. Even though the heat generated from the laser is sufficient to melt the Al substrate (Fig. 5b), the formation of a gap in between the support and substrate (see Fig. 2b) hinders the heat transfer from the support to the substrate, causing the Al-based metallic glass support to experience a lower than the predicted cooling rate. Given that the predicted cooling rates within some parts of the melt pool, e.g. from point II (2.1×10^3 K/s) to III (1.4×10^3 K/s), are close to the R_c, it would not require much reduction in cooling rate for crystallisation to occur, as seen in Fig. 2d.

To further evaluate the interface bond at different substrate temperatures, nanoindentation tests were carried out and the results are shown in Fig. 6. It can be seen that the hardness of the substrate (position 1 to 4) is almost the same for each substrate temperature, suggesting that the substrate far from the interface at 250ºC is not influenced by the convection in the melt pool during the SLM process. At 250ºC, the hardness at the interface (position 5 and 6) is higher than that at room temperature, indicating the formation of a stronger bond at 250ºC. This is probably caused by the composition difference between the sub-circular region at 250ºC (Fig. 4) and the interface region at room temperature. The increase of hardness from Al substrate to metallic glass support is also smoother at 250ºC than room temperature. In addition, the hardness of the metallic glass support also varies between different substrate temperatures. This can be largely attributed to the different thermal histories at different substrate temperatures especially the cooling rates within the metallic glass according to the abovementioned model (Fig. 5) [20, 21]. The lower cooling rates in the melt pool at room temperature cause severe crystallization (Fig. 2b), which is probably the reason for lower hardness at position 9 and 10 at room temperature when compared to 250°C. Similar results have also been reported [11]. As Al is a relatively soft phase compared to Al-based BMG, the increased concentration of Al in the melt pool at 250°C (Fig. 4) could probably lower the hardness at position 7 and 8 when compared to the room temperature. However, to fully understand the variation of hardness in the melt pool at different substrate temperatures, more detailed research work is needed.

4. Conclusions

In summary, it has been shown that substrate temperature plays a critical role in determining the interface bonding between the support and substrate and final solidified microstructures. A higher substrate temperature gives rise to stronger bond and the amorphous nature of the materials is retained. This has been attributed to the high cooling rate and larger melt volume including melting of the Al substrate. The latter is an important condition for enhancing the heat transfer from the support the substrate. Though at the lower substrate temperature the predicted cooling rate is higher, the small melt volume caused a clear boundary and gap to form, in between the support and substrate. This prevents an effective heat transfer from the support to the substrate, resulting in a decrease in the actual cooling rate to below the R_c hence severe crystallization. Therefore, to achieve stronger bonding and avoid crystallization during SLM of metallic glass, using a high substrate temperature is beneficial as long as the cooling rate is kept above the R_c.

Acknowledgements

This work was supported by the Australian Research Council (ARC) Discovery Project DP130103592 and ECM Research Development Grant, The University of Western Australia (UWA). The authors also acknowledge the facilities, and the scientific and technical assistance of the Australian Microscopy & Microanalysis Research Facility at the Centre for

Microscopy, Characterisation & Analysis, The University of Western Australia, a facility funded by the University, State and Commonwealth Governments.

References

[1] Gu DD, Meiners W, Wissenbach K, Poprawe R. Laser additive manufacturing of metallic components: materials, processes and mechanisms. Int Mater Rev. 2012;57:133-64.

[2] Zhang LC, Klemm D, Eckert J, Hao YL, Sercombe TB. Manufacture by selective laser melting and mechanical behavior of a biomedical Ti-24Nb-4Zr-8Sn alloy. Scripta Mater. 2011;65:21-4.

[3] Kanagarajah P, Brenne F, Niendorf T, Maier HJ. Inconel 939 processed by selective laser melting: Effect of microstructure and temperature on the mechanical properties under static and cyclic loading. Mater Sci Eng, A. 2013;588:188-95.

[4] Katakam S, Hwang JY, Paital S, Banerjee R, Vora H, Dahotre NB. In Situ Laser Synthesis of Fe-Based Amorphous Matrix Composite Coating on Structural Steel. Metall Mater Trans A. 2012;43A:4957-66.

[5] Audebert F, Colaço R, Vilar R, Sirkin H. Production of glassy metallic layers by laser surface treatment. Scripta Mater. 2003;48:281-6.

[6] Pauly S, Loeber L, Petters R, Stoica M, Scudino S, Kuehn U, et al. Processing metallic glasses by selective laser melting. Mater Today. 2013;16:37-41.

[7] Li XP, Kang CW, Huang H, Zhang LC, Sercombe TB. Selective laser melting of an $Al_{86}Ni_6Y_{4.5}Co_2La_{1.5}$ metallic glass: Processing, microstructure evolution and mechanical properties. Mater Sci Eng, A. 2014;606:370-9.

[8] Li XP, Kang CW, Huang H, Sercombe TB. The role of a low-energy-density re-scan in fabricating crack-free $Al_{85}Ni_5Y_6Co_2Fe_2$ bulk metallic glass composites via selective laser melting. Mater Des. 2014; 63:407-411.

[9] Mercelis P, Kruth J-P. Residual stresses in selective laser sintering and selective laser melting. Rapid prototyp J. 2006;12:254-65.

[10] Dai K, Shaw L. Thermal and stress modeling of multi-material laser processing. Acta Mater. 2001;49:4171-81.

[11] Li XP, Yan M, Wang JQ, Huang H, Kong C, Schaffer GB, et al. Non-isothermal crystallization kinetics and mechanical properties of $Al_{86}Ni_6Y_{4.5}Co_2La_{1.5}$ metallic glass powder. J Alloys Compd. 2012;530:127-31.

[12] Li XP, Yan M, Yang BJ, Wang JQ, Schaffer GB, Qian M. Crystallization behaviour and thermal stability of two aluminium-based metallic glass powder materials. Mater Sci Eng, A. 2011;530:432-9.

[13] Wang XJ, Zhang LC, Fang MH, Sercombe TB. The effect of atmosphere on the structure and properties of a selective laser melted Al-12Si alloy. Mater Sci Eng, A. 2014;597:370-5.

[14] Roy GG, Elmer JW, DebRoy T. Mathematical modeling of heat transfer, fluid flow, and solidification during linear welding with a pulsed laser beam. J Appl Phys. 2006;100:034903.

[15] Katakam S, Hwang J, Paital S, Banerjee R, Vora H, Dahotre N. In Situ Laser Synthesis of Fe-Based Amorphous Matrix Composite Coating on Structural Steel. Metall Mater Trans A. 2012;43:4957-66.

[16] Abbaschian R, Reed-Hill R. Physical Metallurgy Principles - SI Version: Cengage Learning; 2009.

[17] Weast RC, Selby SM. CRC Handbook of Chemistry and Physics. 60th ed: CTC Press; 1981.

[18] Bergström D. The Absorption of Laser Light by Rough Metal Surfaces. Sweden: Luleå University of Technology; 2008.

[19] Wang WH, Dong C, Shek CH. Bulk metallic glasses. Mater Sci Eng, R. 2004;44:45-89.

[20] Eckert J, Das J, Pauly S, Duhamel C. Mechanical properties of bulk metallic glasses and composites. J Mater Res. 2007;22:285-301.

[21] Loffler JF. Bulk metallic glasses. Intermetallics. 2003;11:529-40.

Figure captions:

Fig. 1 (a) An SEM image and (b) particle size distribution of the $Al_{86}Ni_6Y_{4.5}Co_2La_{1.5}$ metallic glass powder.

Fig. 2 Back-scattered SEM images of the interface between the metallic glass support and the Al substrate with different temperatures: (a) 250ºC; (b) room temperature. (c) and (d) are images corresponding to (a) and the marked areas in (b) at high magnification, respectively. Arrows (in red) point to Al-rich oxide which formed during SLM and arrow (in white) points to unbonded area which forms as a result of insufficient melting during SLM.

Fig. 3 SEM EDS mapping results for elements O and Al in the area shown in Fig. 2a. Arrows (in red) point to Al-rich oxide which formed during SLM. Red is higher in concentration than blue.

Fig. 4 Quantitative chemical maps obtained using EPMA in the sub-circular interface region between the metallic glass support and Al substrate at a substrate temperature 250℃. Only the four major elements Al, Ni, Y, Co are shown here.

Fig. 5 Predicted temperature distribution within the melt pool at different substrate temperatures: (a) 250ºC; (b) room temperature. (c) Cooling rates at different spots (black triangle) within the melt pool, marked by I-V in (a) and (b) at different substrate temperatures. The green line shows the critical cooling rate of this metallic glass.

Fig. 6 (a) Nanoindentation test results showing the variation of hardness from the Al substrate to the metallic glass along the vertical direction at different positions (from 1 to 10) at two substrate temperatures. (b) and (c) are photos showing the positions where indentation experiments were carried out at 250ºC and room temperature, respectively.

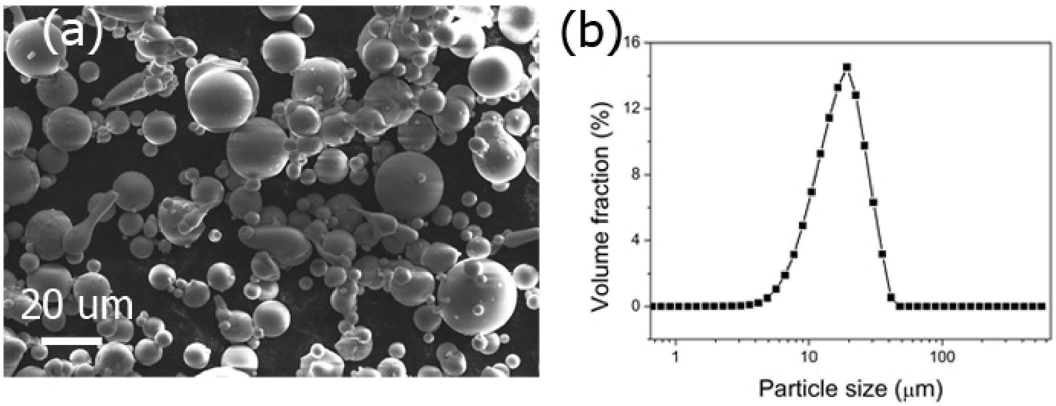
(a)
20 um
(b)
Volume fraction (%)
Particle size (μm)
0
4
8
12
16
1
10
100

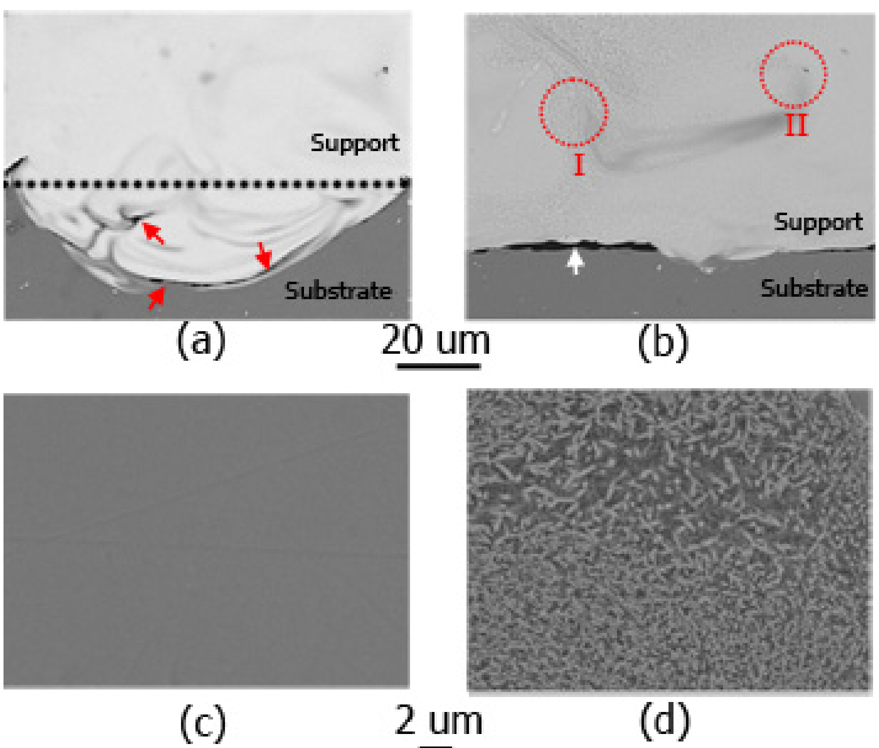
Support
Substrate
I
II
Support
Substrate
(a)
20 um
(b)
(c)
2 um
(d)

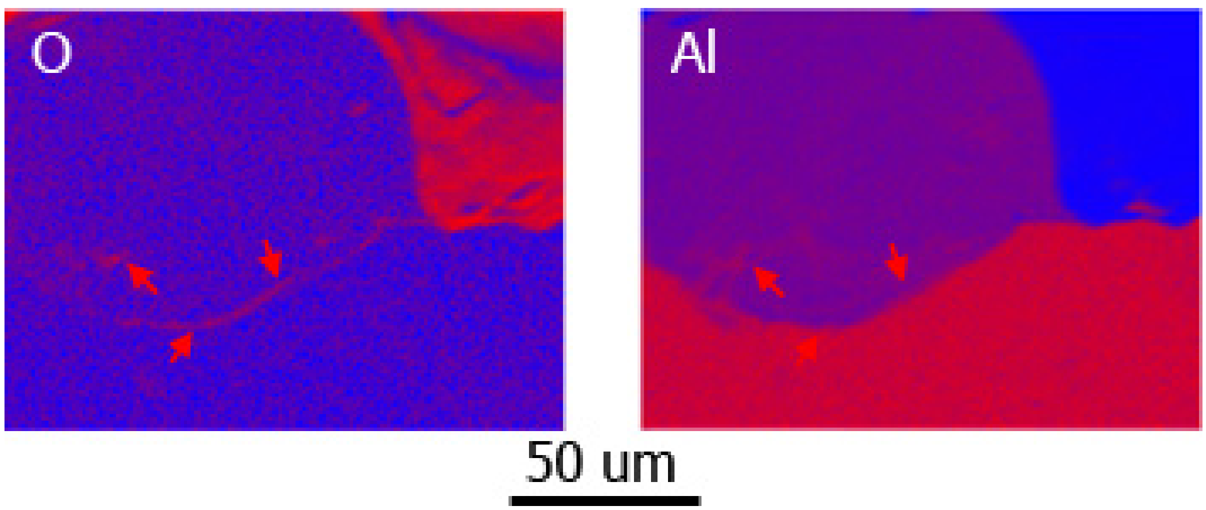
O
Al
50 um

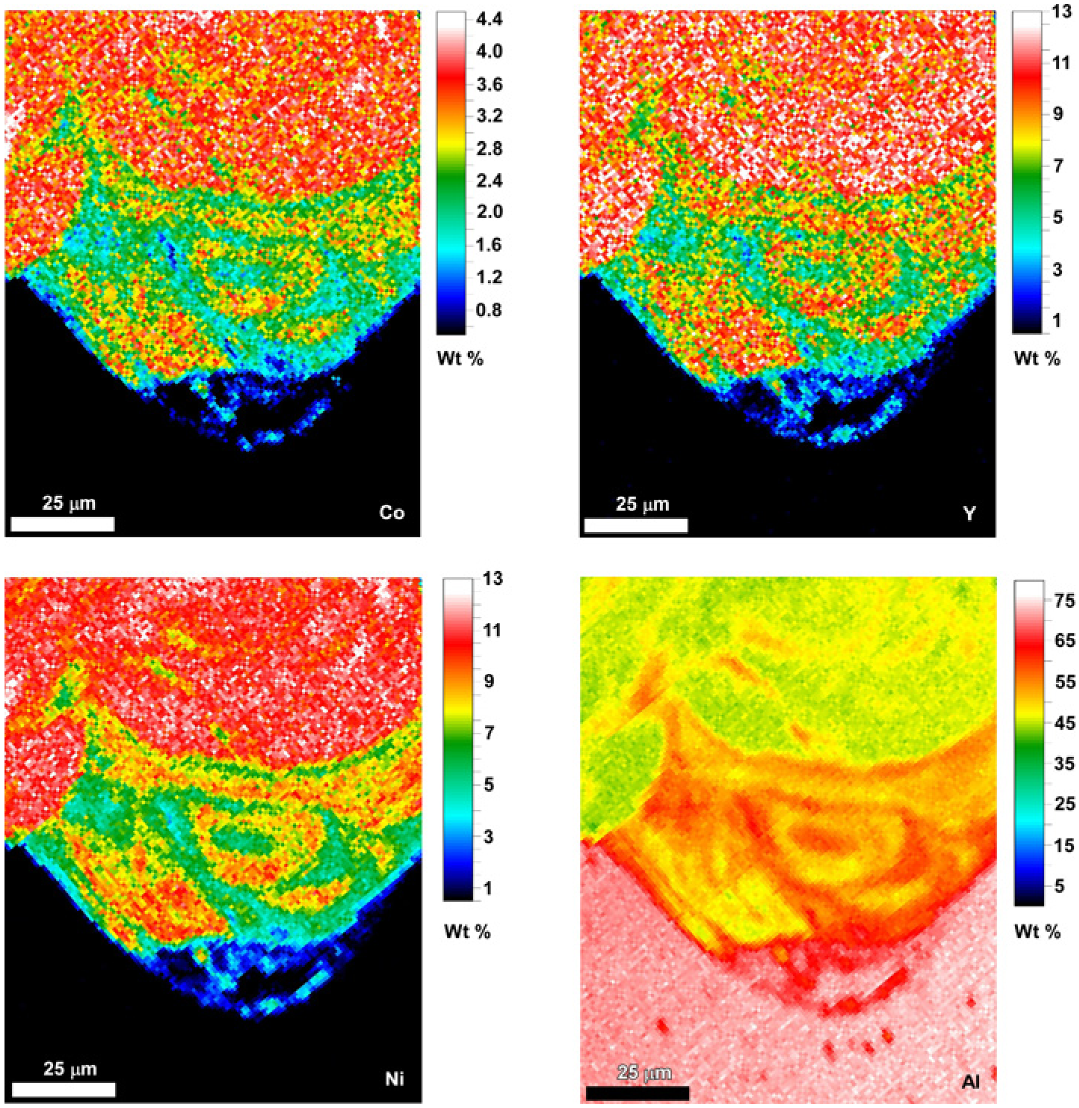
4.4
4.0
3.6
3.2
2.8
2.4
2.0
1.6
1.2
0.8
Wt %
25 μm
Co
13
11
9
7
5
3
1
Wt %
25 μm
Y
13
11
9
7
5
3
1
Wt %
25 μm
Ni
75
65
55
45
35
25
15
5
Wt %
25 μm
Al

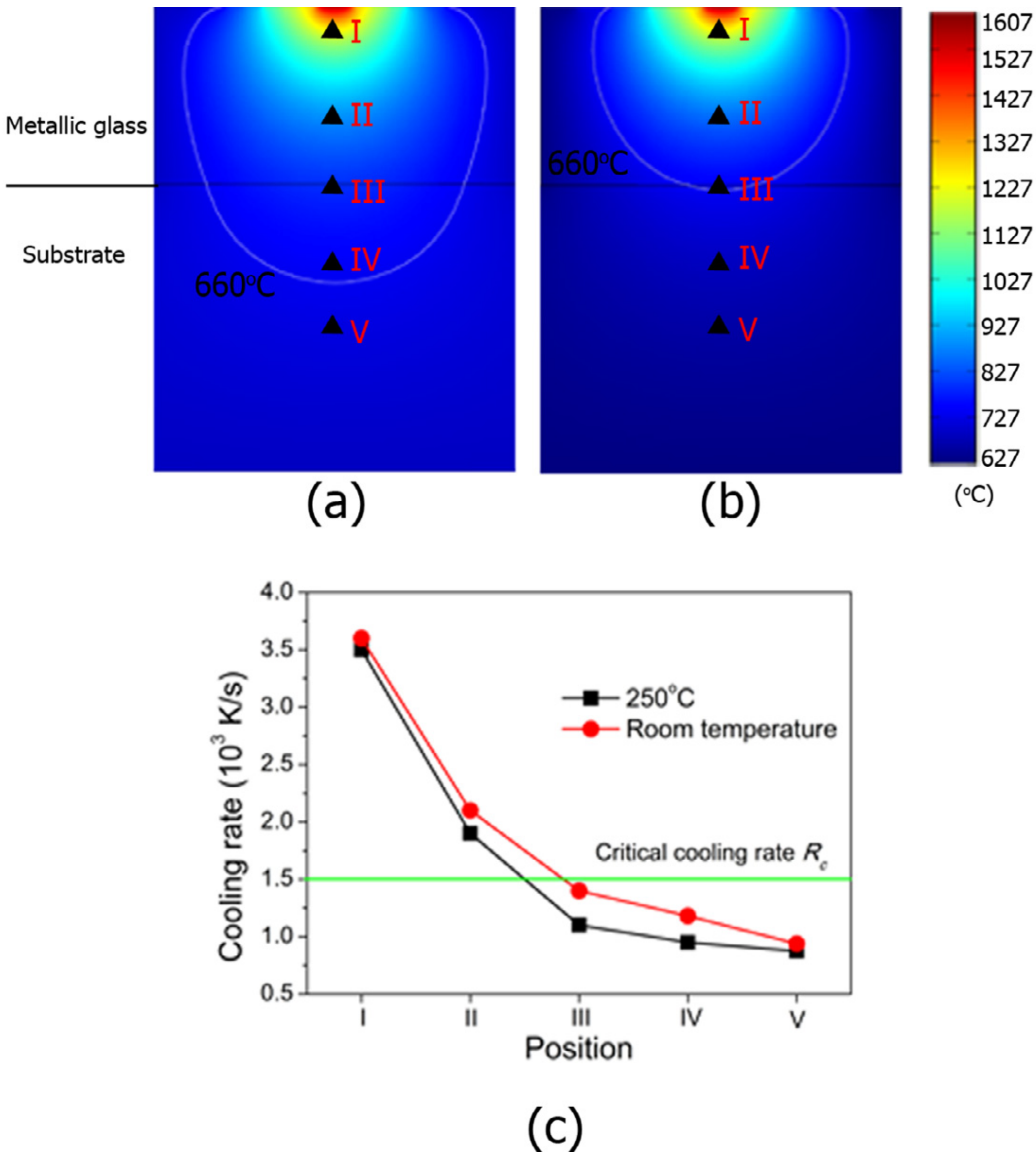
Metallic glass
Substrate
660°C
I
II
III
IV
V
1607
1527
1427
1327
1227
1127
1027
927
827
727
627
(°C)
(a)
(b)
Cooling rate (10³ K/s)
Position
250°C
Room temperature
Critical cooling rate R_c
(c)

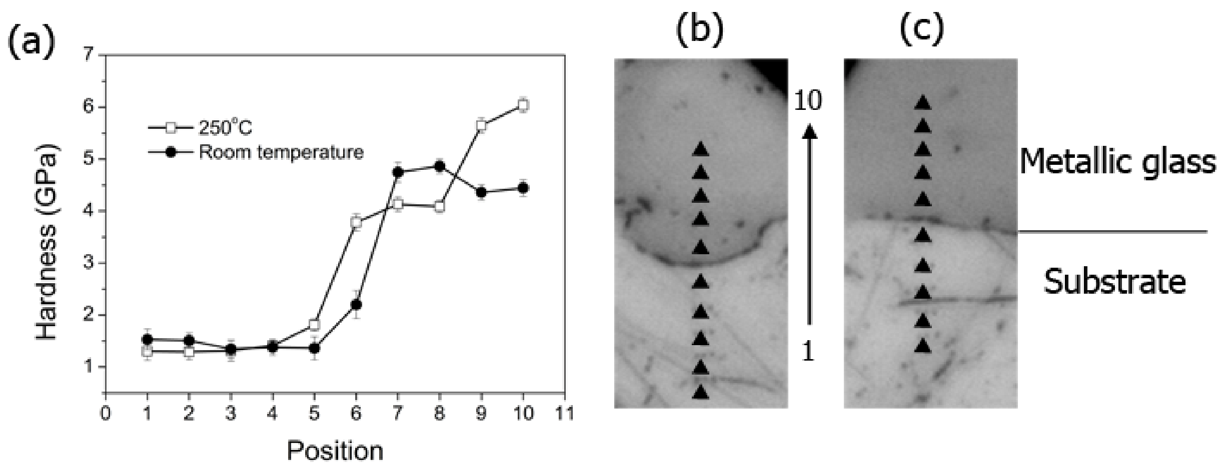
(a)
Hardness (GPa)
Position
250°C
Room temperature
(b)
(c)
10
1
Metallic glass
Substrate

Highlights

- Substrate temperature can influence interface between metallic glass and substrate
- Solidification microstructure is strongly affected by the substrate temperature
- Higher substrate temperature gives rise to a stronger interface bond
- The reason is attributed to different cooling rates and thermal histories